A numerical study on droplet-particle collision:

Lamella characterization

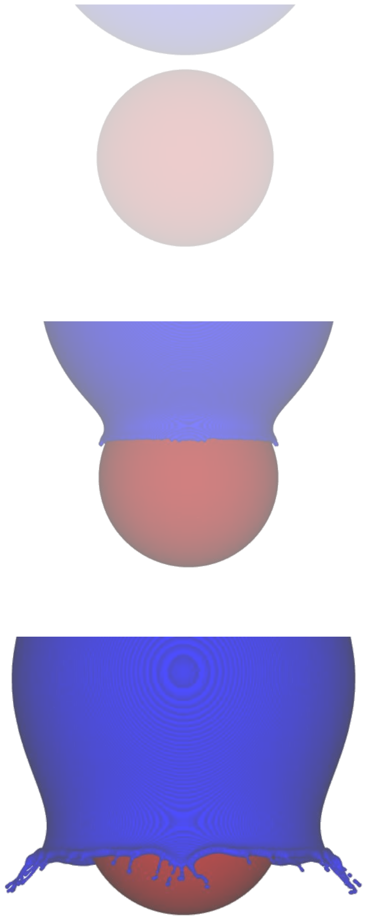

Vitor Vilela
Francisco José de Souza

Scope

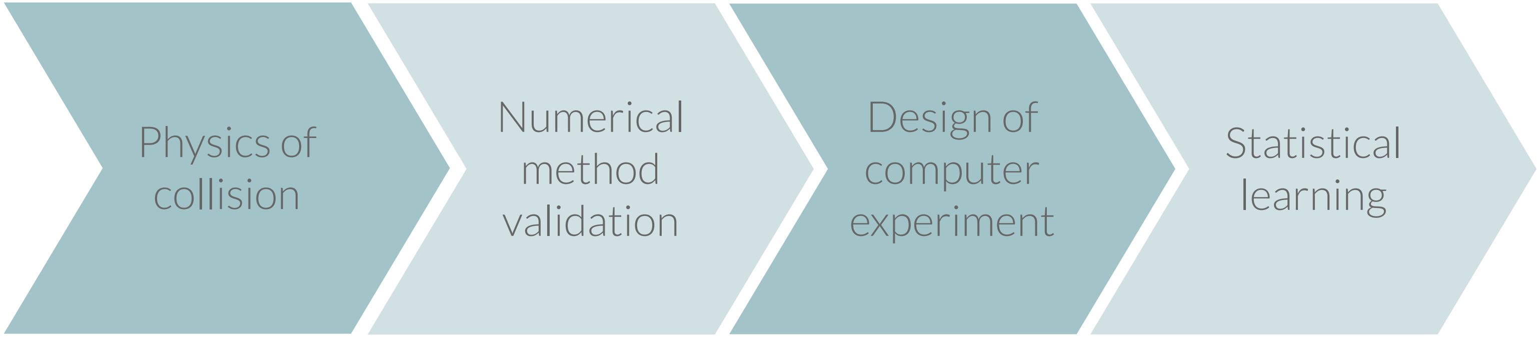

This diagram shows the steps we followed to build a **statistical model** based on detailed Eulerian simulation, which passed through the understanding of the underlying physics of the droplet-particle collision, the **numerical validation**, and the **design of computer experiment**.

Scope

- Physics of collision
- Numerical method validation
- Design of computer experiment
- Statistical learning

In the **physics of collision**, we focused on the **lamella characterization**, particularly related to its deforming area, also presenting a **mechanical energy viewpoint**.

Context

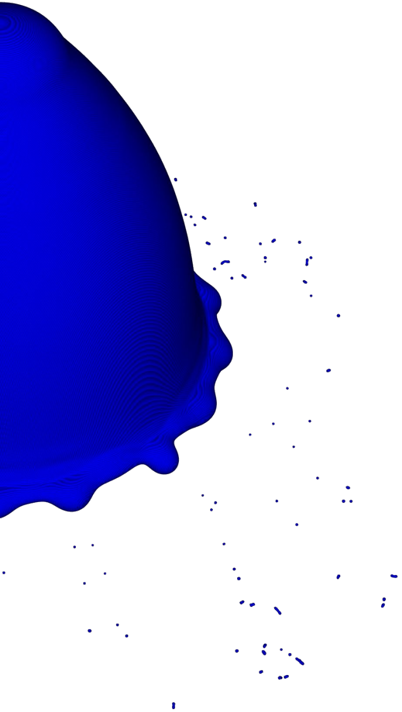

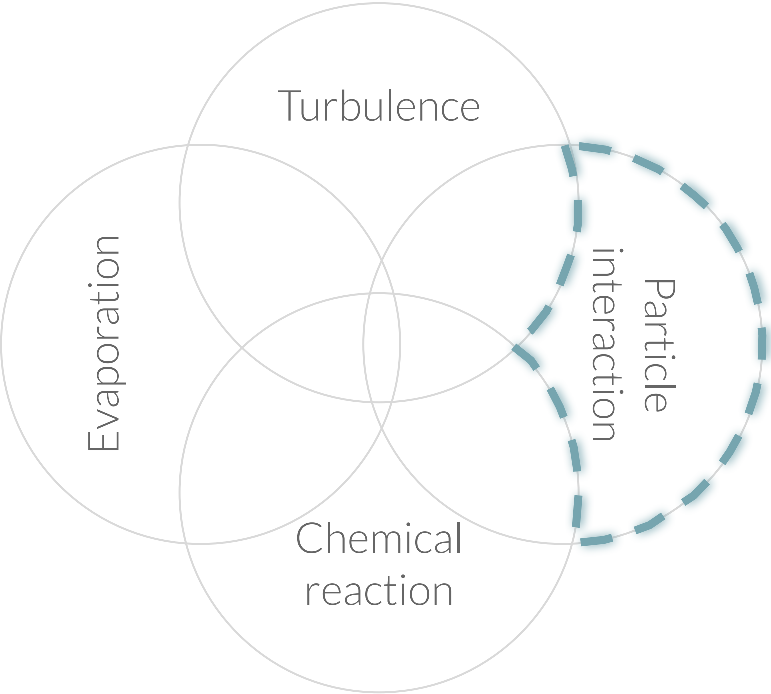

When thinking on the **applications** where we may find **droplets interacting with particles**, we find out that the **real scenario** is much **broader** than what we start modeling on this work. Considering the neighborhood of the droplet, we certainly will have to deal with **turbulence**, which influences the **droplet breakup**.

Context

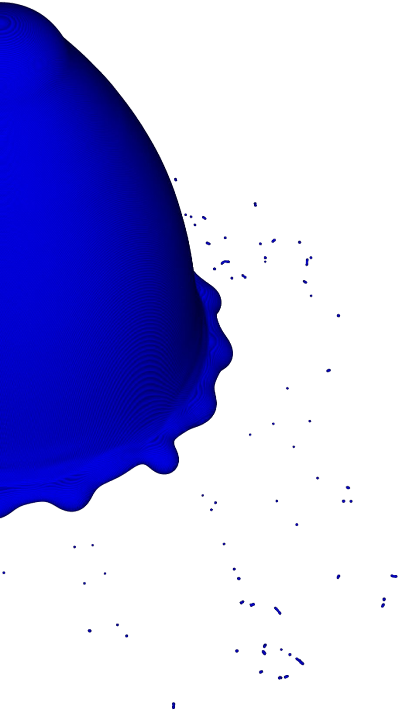

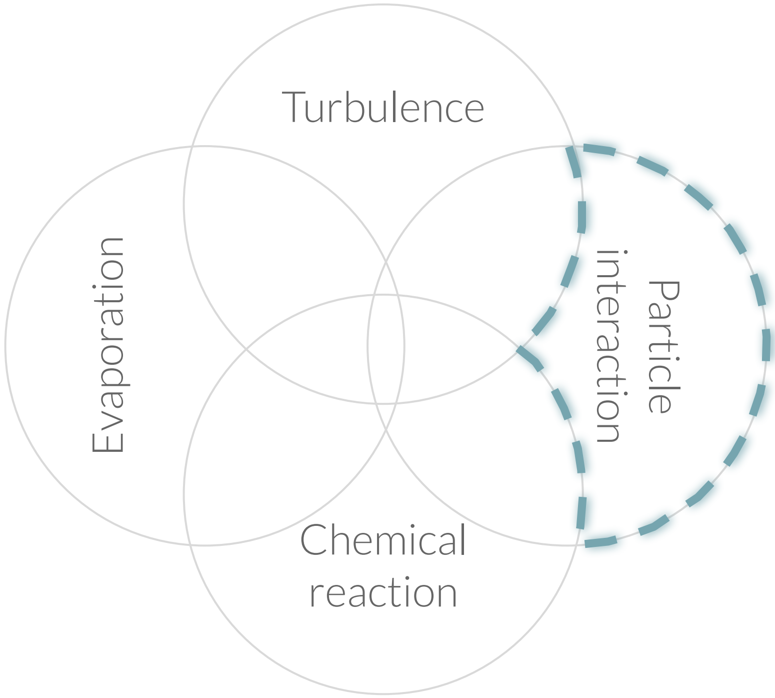

Also, in several industrial processes, a **chemical reaction** may follow the droplet **evaporation**, which brings a new panorama of thermal and chemical phenomena and different numerical modeling issues. Even in **pure particle interaction**, the droplet may collide with a **cluster** of particles or the particle may be **non-spherical** or **porous**.

Physics of collision

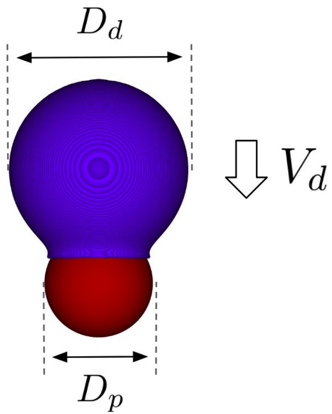

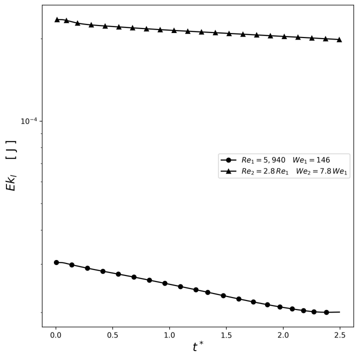

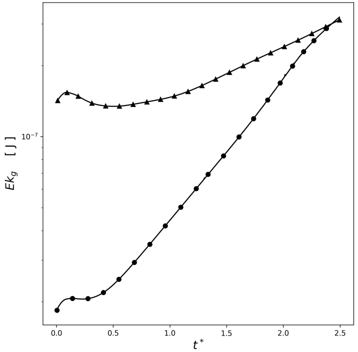

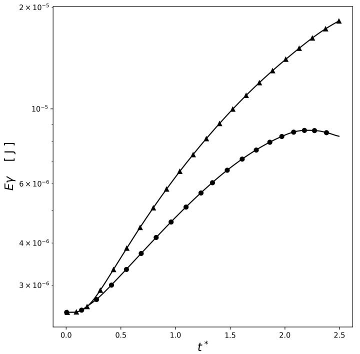

We restricted our analyses to the **isothermal** impact of a single droplet with an aligned, **spherical particle** in an initially **quiescent** environment. **Four** main parameters affect the collision outcomes: First, droplet to particle **diameter ratio**, which we fixed at **1.75**. It is a previously known value that forms **lamella**.

Physics of collision

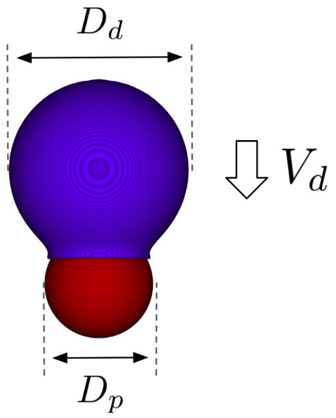

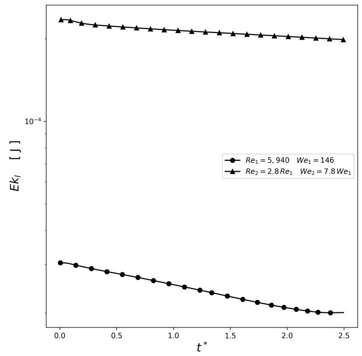

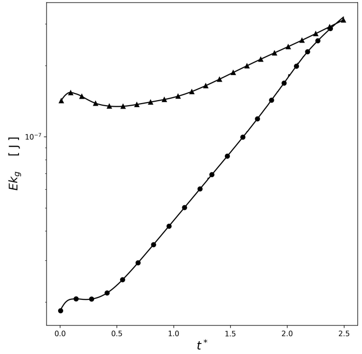

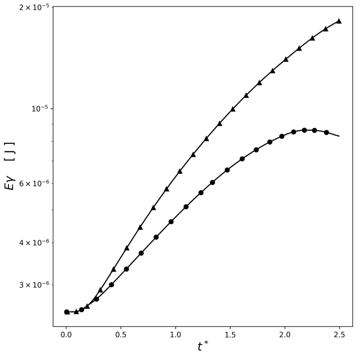

Second, **wetting**, expressed by the **contact angle** dynamics at the triple-point. And finally, **Reynolds** and **Weber** numbers. In this work, we focused on the study of the effects of these parameters on the collision outcomes.

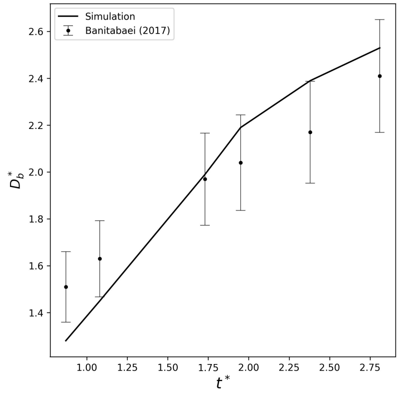

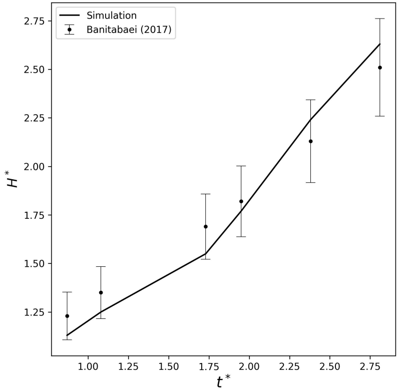

Validation

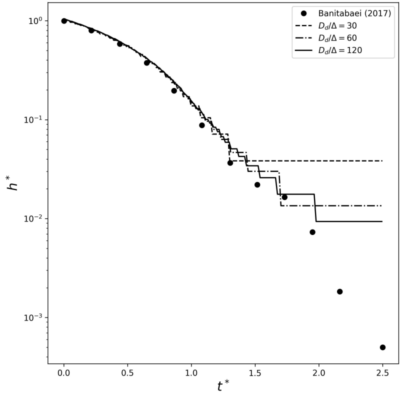

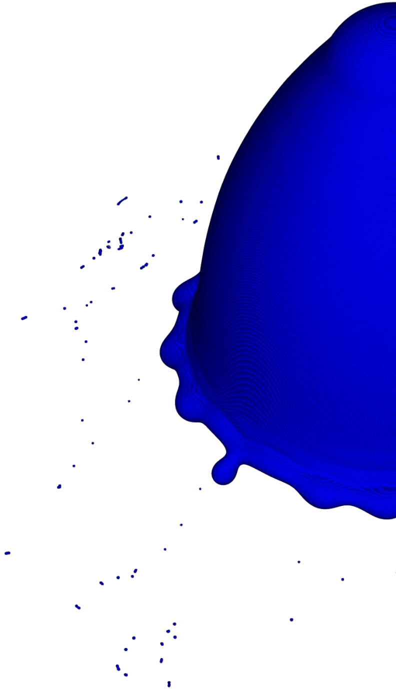

The dimensionless **film thickness** is in good agreement with the experimental data, but it depends on the **level of refinement**. Both the dimensionless lamella **base diameter** and **height** shows agreement within **10%** of the experimental data, but we can improve these results with the modeling of the **contact angle**.

Design of computer experiment

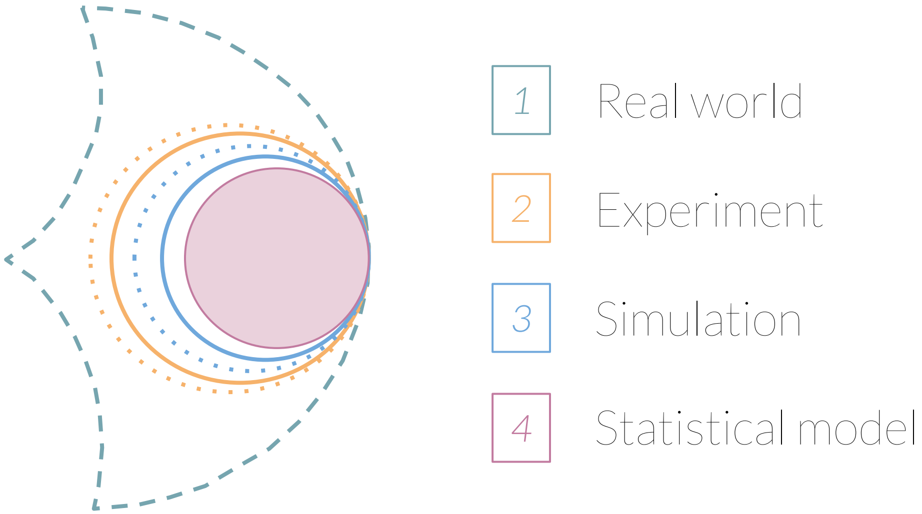

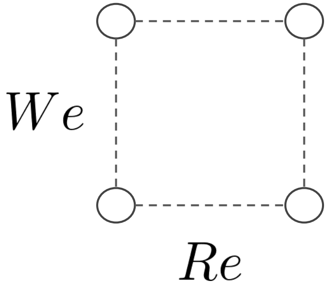

$$CI_{Re} = -0.155 \pm 0.069$$

$$CI_{We} = +0.388 \pm 0.106$$

$$\bar{e} \pm t_{n-1,1-\alpha/2}\sqrt{S^2/n}$$

An **experiment** *#2* differs from the **real world** *#1* by the physical model simplifications and by the **experimental errors**. The design of experiment uses techniques such as blocking and **replicates** to distinguish what is the **effect of the factors** of interest (controlled) and what is the effect of the experimental errors (uncontrolled).

Design of computer experiment

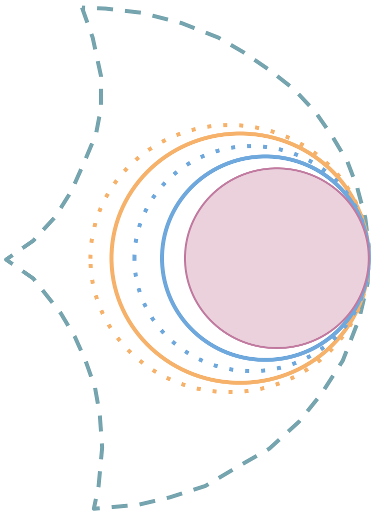

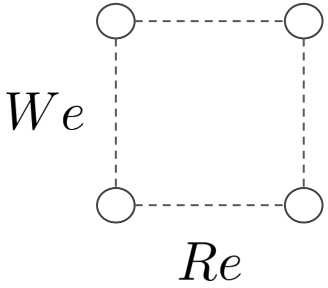

1 Real world

2 Experiment

3 Simulation

4 Statistical model

$$CI_{Re} = -0.155 \pm 0.069$$

$$CI_{We} = +0.388 \pm 0.106$$

$$\bar{e} \pm t_{n-1,1-\alpha/2}\sqrt{S^2/n}$$

A **numerical simulation** *#3* is **deterministic**. The errors come instead, from temporal and spatial **integration schemes**, **grid** and **timestep** size, adopted **models**, etc. Therefore, any **statistical model** *#4* or conclusion built upon simulation results is attached to its specific set of models and parameters. It also presents a **statistical modeling error**.

Design of computer experiment

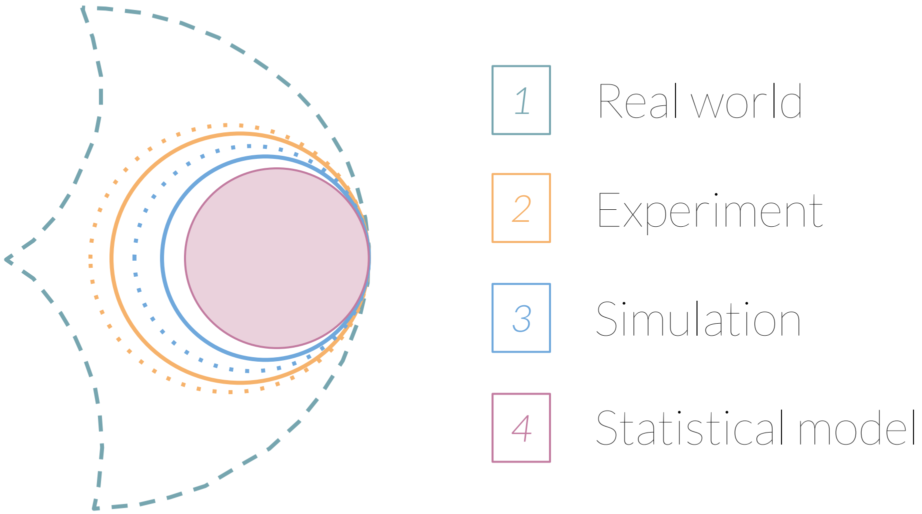

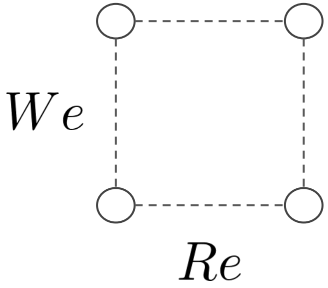

$$CI_{Re} = -0.155 \pm 0.069$$

$$CI_{We} = +0.388 \pm 0.106$$

$$\bar{e} \pm t_{n-1,1-\alpha/2} \sqrt{S^2/n}$$

Design of computer experiment is all about getting the **greater** amount of information from the **minimum data**. Summarizing, **what did we do?**

Design of computer experiment

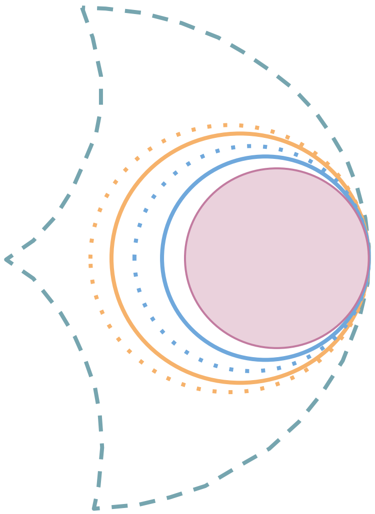

1 Real world

2 Experiment

3 Simulation

4 Statistical model

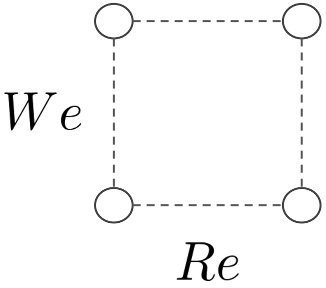

$$CI_{Re} = -0.155 \pm 0.069$$

$$CI_{We} = +0.388 \pm 0.106$$

$$\bar{e} \pm t_{n-1,1-\alpha/2}\sqrt{S^2/n}$$

We evaluated the **effects** of the **Reynolds** number [1,000 - 10,000] and **Weber** number [100 - 1,000] over the **area of the lamella** at **unit dimensionless time** after the droplet impact; and concluded that the **Reynolds** number tends to **decrease** the lamella area, while the **Weber** number tends to **increase** it, confirming our **energetic analysis**.

Design of computer experiment

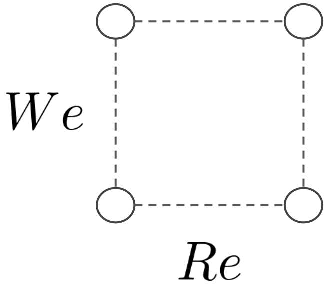

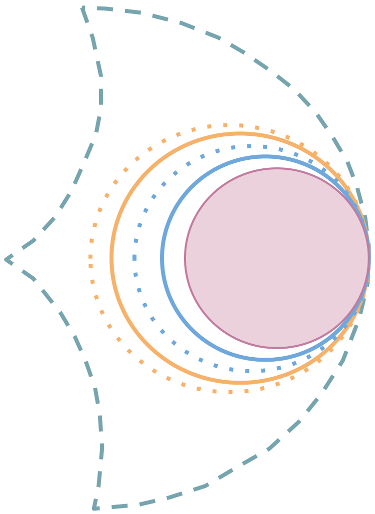

1 Real world

2 Experiment

3 Simulation

4 Statistical model

$$CI_{Re} = -0.155 \pm 0.069$$

$$CI_{We} = +0.388 \pm 0.106$$

$$\bar{e} \pm t_{n-1,1-\alpha/2}\sqrt{S^2/n}$$

We used the **measurable**, but **uncontrolled**, **droplet shape** prior impact reported in the experiment to **mimic** a **replication**. We considered a **spherical** and two different **ellipsoidal shaped** droplets to perform **three replicates** of the factorial design (*n*=3) with a total of **twelve simulations**.

Statistical learning

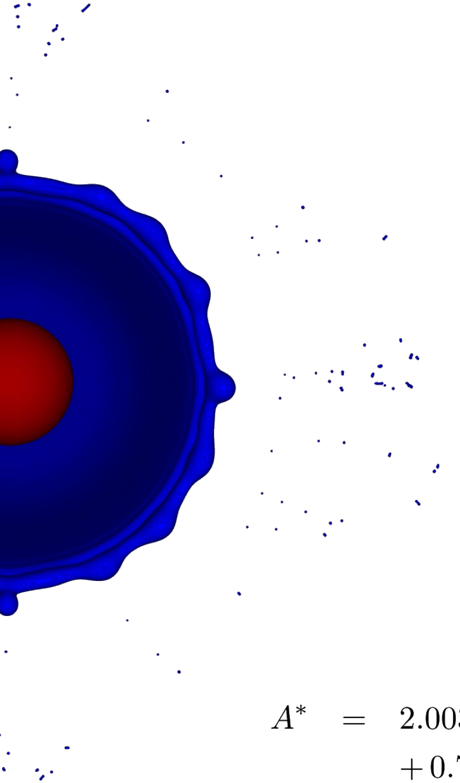

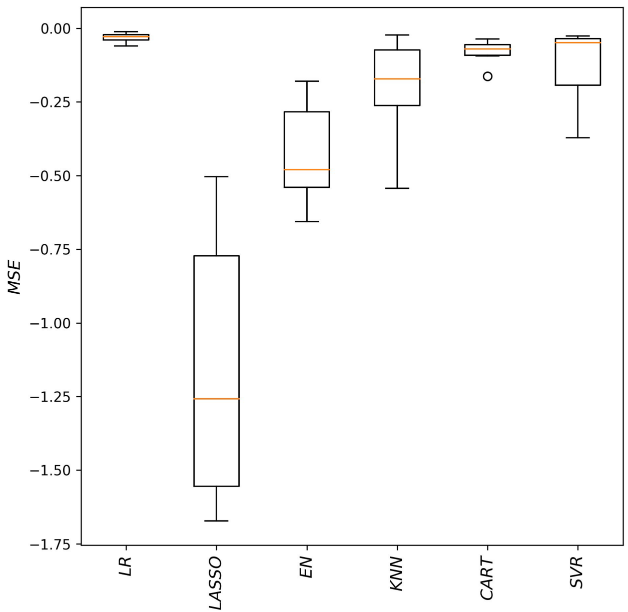

$$
\begin{aligned}
A^* \quad &= \quad 2.003 + 0.385 \cdot \mathrm{Re} + 0.309 \cdot We + 0.041 \cdot t^* - 0.216 \cdot \mathrm{Re}We + 0.282 \cdot t^* We - 0.534 \cdot \mathrm{Re}We^2 \\
&\quad + 0.771 \cdot \mathrm{Re}^2 We - 0.014 \cdot t^* \mathrm{Re}^2 + 0.699 \cdot {t^*}^2 We + 0.397 \cdot \mathrm{Re}^3 + 0.258 \cdot We^3
\end{aligned}
$$

To build a **statistical model** based on the **numerical** results, we simulated a few additional cases in the range of Reynolds and Weber numbers of interest. The **predictive model** for the **dimensionless lamella area** is a function of the **dimensionless time**, **Reynolds** and **Weber** numbers.

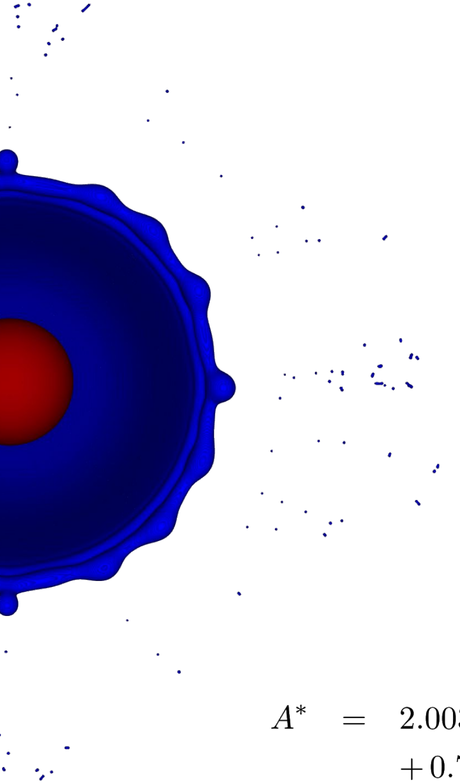

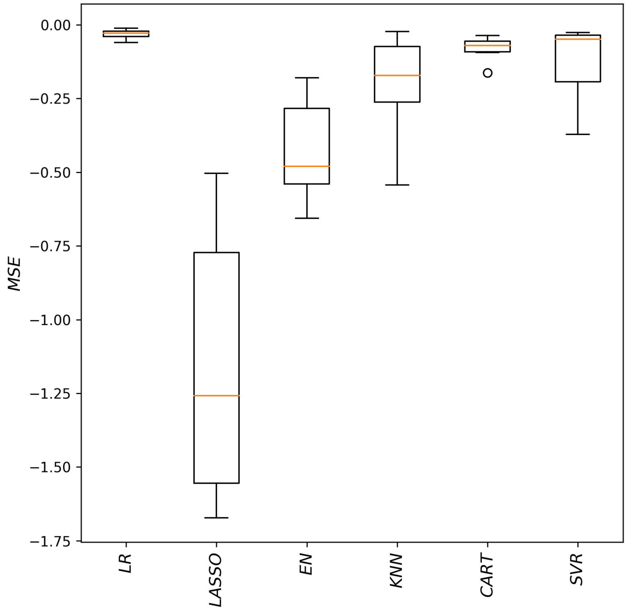

$$
\begin{aligned}
A^* \quad = \quad & 2.003 + 0.385 \cdot \mathrm{Re} + 0.309 \cdot We + 0.041 \cdot t^* - 0.216 \cdot \mathrm{Re}We + 0.282 \cdot t^*We - 0.534 \cdot \mathrm{Re}We^2 \\
& + 0.771 \cdot \mathrm{Re}^2We - 0.014 \cdot t^*\mathrm{Re}^2 + 0.699 \cdot {t^*}^2We + 0.397 \cdot \mathrm{Re}^3 + 0.258 \cdot We^3
\end{aligned}
$$

The box-plot presents the **mean squared error** of some **machine learning** methods, like **polynomial** regressor (a linear model to nonlinear functions) and **decision tree** regressor (a non-linear model to non-linear function).
As a standard practice of **data exploration and modeling**:

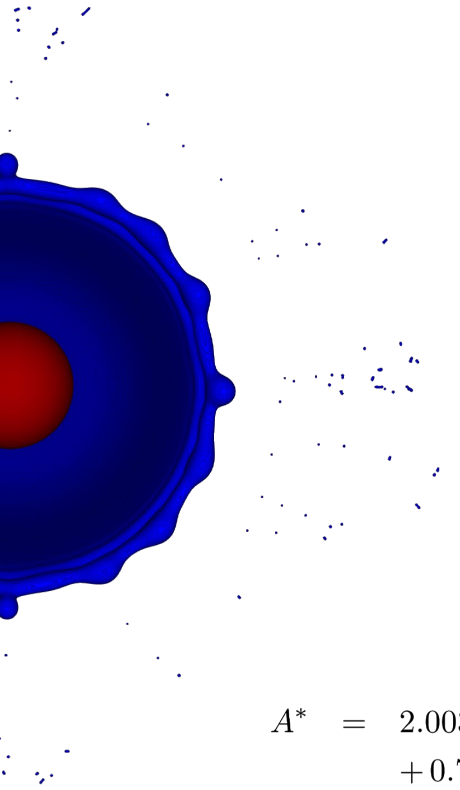

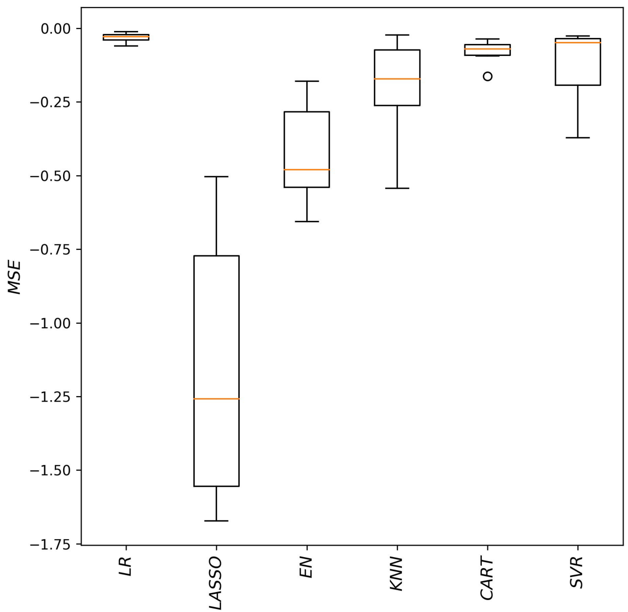

$$
\begin{aligned}
A^* \quad = \quad & 2.003 + 0.385 \cdot \mathrm{Re} + 0.309 \cdot We + 0.041 \cdot t^* - 0.216 \cdot \mathrm{Re}We + 0.282 \cdot t^* We - 0.534 \cdot \mathrm{Re}We^2 \\
& + 0.771 \cdot \mathrm{Re}^2 We - 0.014 \cdot t^* \mathrm{Re}^2 + 0.699 \cdot {t^*}^2 We + 0.397 \cdot \mathrm{Re}^3 + 0.258 \cdot We^3
\end{aligned}
$$

We **divided** our **dataset** into **70%** of **training data** (to fit the model) and **30%** of **test data**.
We **normalized**, subtracting by the mean, and **scaled**, dividing by the standard deviation, all **inputs** based on the training dataset.

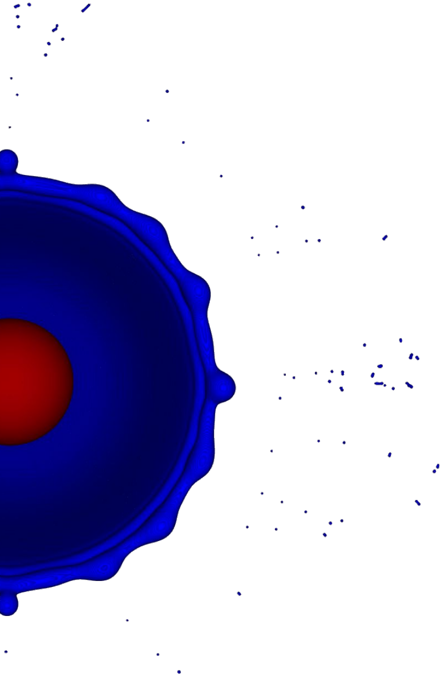

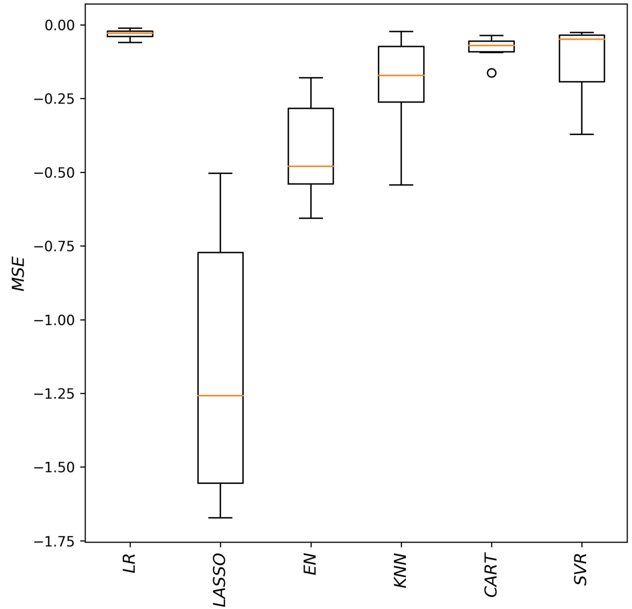

$$
\begin{aligned}
A^* \quad = \quad & 2.003 + 0.385 \cdot \mathrm{Re} + 0.309 \cdot We + 0.041 \cdot t^* - 0.216 \cdot \mathrm{Re}We + 0.282 \cdot t^* We - 0.534 \cdot \mathrm{Re}We^2 \\
& + 0.771 \cdot \mathrm{Re}^2 We - 0.014 \cdot t^* \mathrm{Re}^2 + 0.699 \cdot {t^*}^2 We + 0.397 \cdot \mathrm{Re}^3 + 0.258 \cdot We^3
\end{aligned}
$$

We applied **cross-validation** with **ten** samples to **evaluate** the **MSE** metric of these models based on the test dataset. This 3rd degree **polynomial** model presented the **lower Mean Absolute Percentage Error** of **5.1%**. It receives the **standardized input** variables, with **zero mean** and **unit variance**.

Acknowledgments